Pergamon

Int. J. Solids Structures Vol. 35, Nos 31–32, pp. 4055–4066, 1998

0020–7683/98 $19.00 + .00

PII: S0020–7683(97)00300–4

CRACK PROPAGATION IN CONCRETE COMPOSITES INFLUENCED BY INTERFACE FRACTURE PARAMETERS

ORAL BUYUKOZTURK* and BRIAN HEARING
Department of Civil and Environmental Engineering, Massachusetts Institute of Technology, Cambridge, MA, U.S.A.

(*Received* 22 *November* 1996; *accepted* 3 *June* 1997)

Abstract—The mechanical behavior of concrete composites is influenced by the characteristics of mortar–aggregate interfaces. Initiation and propagation of cracks at the interface or penetration of cracks into the aggregate can greatly influence the global behavior of the material. In the interfacial regions of concrete composites the crack path criterion will involve relative magnitudes of the fracture toughnesses between the interface and the constituent materials. This study investigates fracture of two-phase composites in terms of parameters that influence the cracking scenarios in the interfacial regions and affect the fracture behavior of the concrete. These parameters include elastic moduli mismatch between the mortar and the aggregate and the ratios of the interface fracture toughness to the fracture toughness of the aggregate and the mortar. Numerical and physical model tests were performed to study the influence of these variables on the global load-deformation behavior of composite beams. Physical beam models consisting of circular aggregate inclusions in mortar matrices were tested in three-point bending. An analysis capability is developed for cracking in the composite incorporating transgranular or interfacial fracture scenarios using finite element simulations performed with the material fracture properties. The simulation is of a cohesive force type that allows parametric variation of fracture parameters to study influences on load-deformation performance of the composite. Results of the simulation are used to quantify the effect of different interfacial properties on the fracture and load-deformation behavior of the specimens. The results of both the experimental and analytical model studies show that ductility improves when cracks propagate through mortar–aggregate interfaces and also improves with rougher aggregate surfaces. This study advances the understanding of the role of interfaces in the global behavior of the cementitious composites and furthers the development of high-performance cementitious materials.

INTRODUCTION

The use of high strength concrete for improved structural performance in infrastructure development and renewal around the world continues to increase. A concern with this increased use is the brittle nature of failure of high strength concrete compared to the relatively ductile failure of normal strength concrete; this concern has limited the application of high strength concrete in flexural members where its advanced performance capabilities would be advantageous. For this reason, interest in the fracture behavior of cementitious composites has increased with the need for the development of high performance concrete with improved toughness and ductility.

The development of bond cracks at mortar–aggregate interfaces is an important factor in the inelastic deformation and fracture behavior of concrete (Hsu *et al.*, 1963; Shah and Winter, 1966; Buyukozturk *et al.*, 1971). Bond cracks in normal strength concrete often propagate along the interface between mortar and aggregate, absorbing energy before linking and forming continuous cracks through mortar at failure. In this respect the fracture properties of the interface relative to the mortar are important parameters that affect the global material behavior. In higher strength concretes, however, the interface zones have been shown to be more dense and stronger than interfaces in normal strength concrete, often preventing the formation of the interfacial bond cracks and facilitating stress transfer to weaker aggregate particles (Lee *et al.*, 1992; Chatterji and Jensen, 1992; Trende and Buyukozturk, 1995; Buyukozturk and Lee, 1993). Crack propagation through aggregates has been observed in high strength concrete, indicating a less pronounced effect of crack

* Author to whom correspondence should be addressed. E-mail: obuyuk@mit.edu.

arrest by aggregates and more brittle global material behavior (Carrasquillo *et al.*, 1981; Gerstle, 1979). Here, the fracture properties of the aggregate relative to the mortar are important parameters affecting the performance of the material. In the improvement of the performance of high strength cementitious materials a fundamental understanding and quantitative data with respect to the influence of these interface, aggregate, and mortar fracture properties on the material behavior is necessary.

In this study the authors investigate the influence of mortar, aggregate, and interfacial fracture properties on the performance of concrete composites. Relative fracture parameters and how they affect the behavior and ductility of the composite are studied in a combined experimental and analytical research program. For this, physical models with combinations of mortar, aggregate, and interfacial fracture parameters are tested through mortar beams with embedded circular aggregate inclusions. Analytical models are employed to simulate the fracture process of the tested physical specimens during failure. The models are used in parametric studies to investigate the influence of relative fracture properties of the mortar, aggregate, and interface on the deformation behavior of the composite.

CRACK PROPAGATION AT MORTAR–AGGREGATE INTERFACES

It has been suggested that the mechanical properties of concrete are largely attributable to the properties of mortar–aggregate interface regions (Goldman and Bentur, 1989; Lee and Buyukozturk, 1994). Quantitative studies of interfacial fracture processes through interface fracture mechanics concepts (Rice, 1988) offer great potential for the understanding of the global material behavior of concrete. The main objectives of interface fracture mechanics are to define and assess the fracture energy release rate of interfaces and also to quantify fracture criteria for crack path prediction.

The energy release rate G per unit length of extension of a crack at an interface in a bimaterial system is related to the stress intensity factors with an Irwin-type relation

$$G = \frac{|K|^2}{E^* \cosh^2 \pi\varepsilon} \tag{1}$$

where $|K|^2 = K_1^2 + K_2^2$ is the sum of the squares of the mode I and mode II stress intensity factors, E^* is an average stiffness defined by

$$\frac{1}{E^*} = \frac{1}{2}\left(\frac{1}{\bar{E}_1} + \frac{1}{\bar{E}_2}\right) \tag{2}$$

$\cosh^2 \pi\varepsilon = 1/(1-\beta^2)$, and $\bar{E}_i = E_i/(1-\nu_i^2)$ is the plane strain elastic modulus for material i. The complex interface stress intensity factor $K = K_1 + iK_2$ has a real and imaginary parts K_1 and K_2 which are similar to conventional mode I and mode II intensity factors in a homogeneous solid. Bimaterial elasticity depends on two moduli mismatch parameters α and β defined by (Dundurs, 1969)

$$\alpha = \frac{\bar{E}_1 - \bar{E}_2}{\bar{E}_1 + \bar{E}_2} \quad \beta = \frac{1}{2}\frac{\mu_1(1-2\nu_2) - \mu_2(1-2\nu_1)}{\mu_1(1-\nu_2) + \mu_2(1-\nu_1)} \tag{3}$$

where μ_i and ν_i represent the shear modulus and Poisson's ratio of material i.

The energy release rate G is defined as a function of the real phase angle $\hat{\psi}$ of the stress intensity factors ahead of the crack tip

$$\hat{\psi} = \arctan\left(\frac{\Im(KL^{i\varepsilon})}{\Re(KL^{i\varepsilon})}\right) \tag{4}$$

where L is a somewhat arbitrary reference length and $\varepsilon = (1/2\pi)\ln[(1-\beta)/(1+\beta)]$. Here $\hat{\psi}$

measures the relative proportion of the effect of mode II to mode I stresses on the interface. For many practical systems, including mortar–aggregate interfaces, the effect of nonzero β is often the secondary consequence, reducing the phase angle $\hat{\psi}$ to

$$\hat{\psi} = \arctan\left(\frac{K_2}{K_1}\right) \tag{5}$$

Fracture energy release rates for a variety of mortar–aggregate interfaces have been assessed through sandwich beam and Brazilian disk specimen tests (Buyukozturk and Lee, 1993; Lee *et al.*, 1992). As an example, an interface fracture energy curve for a high strength mortar–granite aggregate interface is given in Fig. 1. It is observed that the interfacial fracture energy markedly increases as the loading phase angle increases. Similar trends were found in both normal and high strength mortar–aggregate interfaces with greater fracture energies exhibited by the high strength mortar (Lee *et al.*, 1992). Rougher aggregate surfaces have also been shown to increase the interfacial fracture energy (Trende and Buyukozturk, 1995).

In concrete, a crack impinging a mortar–aggregate interface has been shown to advance by either penetrating into the aggregate or deflecting along the interface (Buyukozturk, 1993). Let Γ_i be the toughness of the interface as a function of $\hat{\psi}$ and let Γ_1 be the mode I toughness of the aggregate. The impinging crack is likely to be deflected (He and Hutchinson, 1989) if

$$\frac{\Gamma_i}{\Gamma_1} < \frac{G_i}{G_a^{\max}} \tag{6}$$

where Γ_1 and Γ_i are material properties, which can be measured by fracture testing, and G_i is the energy release rate of the crack deflected into the interfaces, and $G_a^{\max}$ is the maximum energy release rate of the crack penetrating into the aggregate. For complex geometries the ratio $G_i/G_a^{\max}$ can be calculated using numerical analyses schemes (Romeo and Ballarini, 1995), but the ratio has been analytically computed for semi-infinite crack problems (He and Hutchinson, 1989). It was found that with the crack approaching perpendicular to the interface, G_i/G_a is equal to approximately 1/4, indicating that the crack will deflect if the interface toughness is less than a quarter of the aggregate.

From eqn (6) is it shown that the fracture energy of the interface relative to that of the aggregate can shift the fracture processes in concrete from interfacial to aggregate penetration, which can subsequently alter the global behavior of the material during failure.

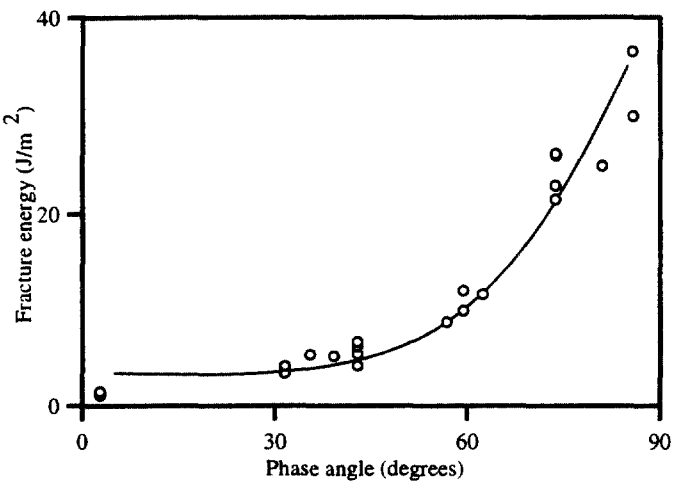

Fig. 1. Fracture energy curves of mortar–aggregate interfaces.

However, little is known about the quantitative influence this shift can have on the behavior of concrete. Furthermore, the influence of variations in these fracture parameters on the behavior of the fracture process is not widely known. For this reason, composite specimens with strong and weak aggregates were tested with different interfaces and mortars to study these influences.

EXPERIMENTAL PROCEDURE

Physical models of two-phase cementitious composites were tested to study crack penetration and deflection at mortar–aggregate interfaces. Two types of circular inclusion beam specimens shown in Fig. 2 were tested under three-point bending to investigate concrete fracture as a composite. The dimensions of the single inclusion specimen were $300 \times 75 \times 25$ mm and the double inclusion specimen were $228 \times 75 \times 25$ mm. Two different mortar strengths were used with circular inclusions of granite and limestone placed along the crack path in three-point bending specimens with a notch created in the mortar below the inclusion.

The testing parameters in this study were the mortar strength, the aggregate strength, and the interfacial fracture resistance. Variations in interfacial energy were achieved through smooth and sandblasted aggregate surface roughnesses and different material combinations. All specimens were made using Type III cement to produce high early strength mortars. Compression strength and elastic modulus tests on the materials were performed with compression cylinders. Tensile strengths were measured using splitting cylinders and fracture energies were measured with three-point bending tests. The properties of the materials are reported in Table 1. All specimens were tested after seven days of curing. Three-point bending tests on the beam specimens were performed using an Instron machine with a loading head displacement control of 0.075 mm/min. During the testing, the ultimate loads and load and load-line displacement signals were recorded to measure the bending performance of the specimens.

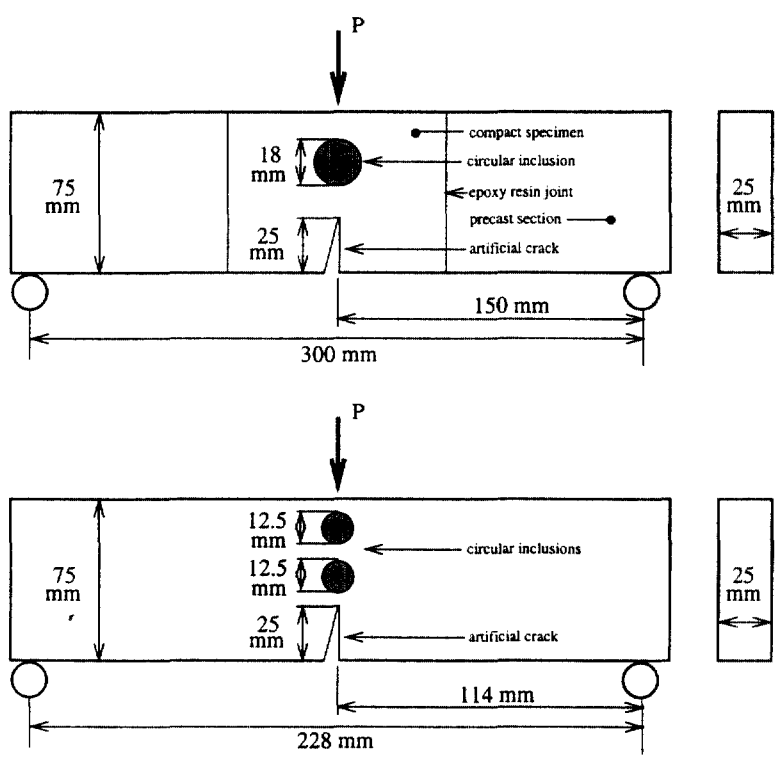

Fig. 2. Three-point bending loading used on circular inclusion specimens.

Table 1. Material properties

Material	σ_c [MPa]	σ_t [MPa]	E [GPa]	ν	G_f [J/m^2]
Low strength mortar	40.0	2.8	27.8	0.2	39.0
High strength mortar	83.8	5.0	33.3	0.2	57.0
Granite	123.0	6.2	42.2	0.16	59.7
Limestone	57.5	3.1	34.5	0.18	29.2

Table 2. Fracture loads of the tested specimens

Series	Type of aggregate	Number of inclusions	Mode of failure	P_u^{avg} [kN]
Low strength/smooth	Granite	1	Interfacial	0.6150
High strength/smooth	Granite	1	Interfacial	0.6377
Low strength/sandblasted	Granite	1	Interfacial	0.6364
High strength/sandblasted	Granite	1	Interfacial	0.6655
Low strength/smooth	Limestone	2	Transgranular	0.6802
Low strength/smooth	Granite	2	Interfacial	0.6837
High strength/smooth	Limestone	2	Transgranular	0.9344
High strength/smooth	Granite	2	Interfacial	1.1395

Results of experimental program

Average failure loads P_u^{avg} for the laboratory tests are reported in Table 2. Specimens with granite inclusions failed with interfacial crack propagation as illustrated in Fig. 3(a) and specimens with limestone failed with transgranular aggregate penetration as illustrated in Fig. 3(b). Failure loads of specimens with interfacial failure were found to increase with high strength mortar and also increase with rougher aggregate surfaces. Load/load-line displacement curves for samples of the specimens with one granite inclusion are shown in Fig. 4(a). Peak loads are shown to increase with greater mortar strength; additionally, specimens with normal strength mortar exhibited a secondary peak lower than an initial first peak, while specimens with higher strength mortars demonstrated a higher secondary peak. The secondary peaks exhibited by the systems may indicate the occurrence of specimen fracture processes; the secondary peaks may be caused by the increase in fracture resistance as the crack deflects out of the interface back into the tougher mortar. Specimens with sandblasted aggregate are also shown to have higher load magnitudes with similar peaking behavior. These effects may be due to increased fracture resistance found in high strength mortar interfaces and rougher aggregate surfaces (Lee *et al.*, 1992; Trende and Buyukozturk, 1995).

(a) Failure modes with granite inclusions (b) Failure mode with limestone inclusio

Fig. 3. Sample failure modes of tested specimens.

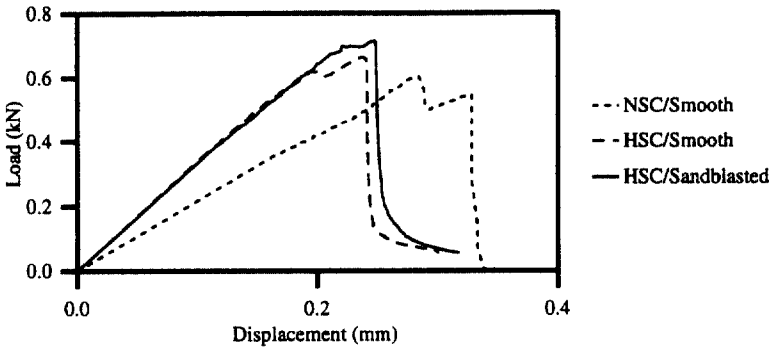

(a) Single circular inclusion specimens

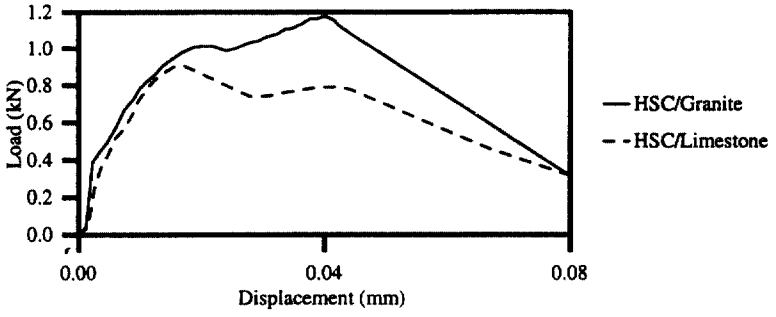

(b) Double circular inclusion specimens

Fig. 4. Experimental load/load-line deflection diagrams.

Failure loads of specimens with transgranular failure are also found to increase with mortar strength; however, their peak loads were lower than specimens with interfacial failure. Load/load-line displacement curves for a sample specimen with two limestone inclusions that resulted in transgranular failure is compared to a sample specimen with two granite inclusions that resulted in interfacial failure in Fig. 4(b); peak loads for the granite specimen is 22% higher than the limestone specimen. It is seen that failure loads of all specimens with limestone inclusions that resulted in transgranular aggregate failure are lower than failure loads of specimens with granite. This may be due to a decreased effect of crack arrest mechanism and differences in fracture energies of the aggregates compared to the interface.

The results of the experimental testing of the inclusion specimens demonstrated the sensitivity of composite behavior to different constituent and interfacial properties. The composite performance can change with shifts in the fracture processes from interfacial to transgranular crack propagation. This behavior can be verified through the crack path criteria given by eqn (6). The phase angle $\hat{\psi}$ for the crack as it approaches the aggregate inclusion in the three-point bending specimen has been calculated by finite element analysis (Buyukozturk and Hearing, 1996b). Interfacial fracture energies for the mortar–aggregate combinations and surface roughnesses used in the tests have been investigated (Lee *et al.*, 1992; Trende and Buyukozturk, 1995) and are shown in Table 3. The ratios $G_i/G_a^{\max}$ are computed from tables (He and Hutchinson, 1989) and are also shown in Table 3. The ratios given by eqn (6) predict interfacial failure for the granite inclusion specimens and aggregate penetration for the limestone inclusion specimens, agreeing with the results of the experimental program and demonstrating the significant influence that constituent properties can have on composite behavior.

Table 3. Verification of prediction criteria

Series	Γ_i [J/m^2]	Γ_i/Γ_1	G_d/G_p^{max}	Predicted mode	Actual mode
Normal strength/smooth granite	22.0	0.37	0.39	Interfacial	Interfacial
Normal strength/sandblasted granite	22.5	0.38	0.40	Interfacial	Interfacial
High strength/smooth granite	20.0	0.33	0.34	Interfacial	Interfacial
High strength/sandblasted granite	21.0	0.35	0.35	Interfacial	Interfacial
Normal strength/limestone	22.0	0.75	0.30	Transgranular	Transgranular
High strength/limestone	18.0	0.62	0.26	Transgranular	Transgranular

From the results of the tests it is concluded that the behavior of the specimens with interfacial crack propagation are affected by the fracture toughness of the interface. In specimens with aggregate penetration it is concluded that the behavior is affected by the fracture resistance of the aggregate. To understand the effects of these factors and to assess their influence on the behavior of the specimens, an analytical procedure is presented.

NUMERICAL PROCEDURE

To further assess the influence these constituent and interfacial fracture properties have on the performance of the composite as a whole, a numerical investigation was conducted. Two separate cohesive force models were used to simulate the interfacial propagation and aggregate penetration fracture processes in the tested samples. Cohesive force models use linear elastic fracture mechanics (LEFM) to simulate material fracture process zones with fictitious cohesive forces trailing a crack tip in equilibrium with external forces (Hillerborg *et al.*, 1976). For example, the forces used in the interfacial propagation model are shown in Fig. 5. A stress intensity superposition is utilized to combine mode I and mode II stresses with the external three-point bending load to calculate mode I and mode II crack opening displacements. The strain–softening constitutive relationship of the material determines the cohesive forces in the fracturing material behind the crack tip. It has been concluded that a bilinear strain–softening relationship best models fracture in most concretes, mortars, and aggregates, and that a linear strain–softening relationship best models fracture in mortar–aggregate interfaces (Buyukozturk and Hearing, 1996a; Foote *et al.*, 1986). Figure 6 shows the relationships that are used to relate cohesive forces with crack opening displacements during fracture.

Finite element investigation

Implementation of a cohesive force model requires an integration of stress intensity factors for a series of crack propagation steps that represent a discretization of fracture. Each of these "steps" will represent the geometry of a hairline crack along the crack path to the ending point of the crack. Stress intensity factors for the simulation with aggregate penetration were available from simple three-point bending relationships (Tada *et al.*,

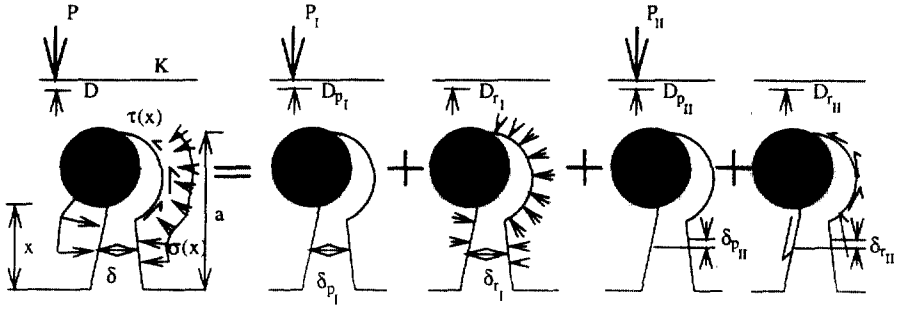

Fig. 5. Stress intensity superposition for circular inclusion specimens.

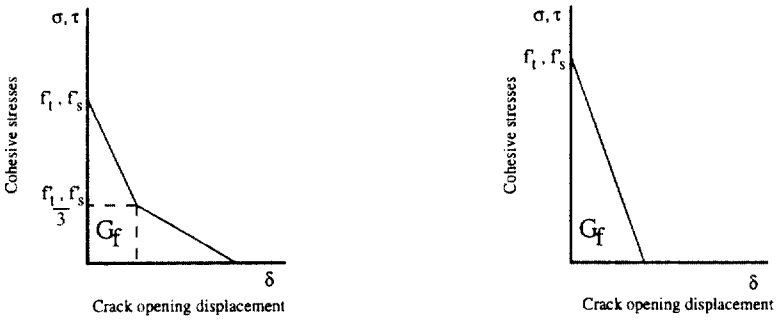

Fig. 6. Bilinear and linear constitutive models.

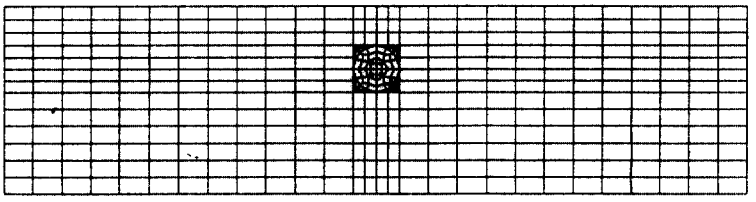

Fig. 7. Finite element discretization of the circular inclusion specimen.

1985). However, for the interfacial fracture model stress intensity factors for a circular inclusion were not readily available and a finite element stress intensity factor investigation was conducted.

The circular inclusion specimen was discretized with 16 nodes radially around the circumference of the inclusion, as shown in Fig. 7. Solutions of this mesh with various permutations of cohesive and external forces were conducted to obtain mixed-mode stress intensity factors. A displacement extrapolation routine was implemented (Owen and Fawkes, 1983) and modified to calculate stress intensity factors at interfacial crack tips. The results were used in the interfacial fracture simulation.

Cohesive fracture models

Using two separate iterative computer models, simulated load/load-line displacement diagrams of the tested specimens with interfacial fracture and aggregate penetration are generated. The relation between load and load-line displacement is obtained by solving the equations of the net stress intensity factor (K_c), the equilibrium of crack opening displacement (COD) at the crack surface, and the constitutive function of the COD and cohesive stresses. The crack opening displacements are calculated by a K-superposition method. Figure 5 shows that in the interfacial specimens there are four contributions to K_c. Two are the stress intensity factors due to the applied load (P), K_{P_I} and $K_{P_{II}}$; the others, K_{r_I} and $K_{r_{II}}$, are due to the tensile cohesive forces $\sigma(x)$ and the shear cohesive force $\tau(x)$ acting across the crack faces in the process zone.

$$K_c = (K_{P_I} + K_{r_I}) + i(K_{P_{II}} + K_{r_{II}}) \tag{7}$$

The equilibrium of crack opening displacement at the crack surface is given by

$$\delta = (\delta_{P_I} + \delta_{r_I}) + i(\delta_{P_{II}} + \delta_{r_{II}}) \tag{8}$$

where δ_{PI} and δ_{PII} are the CODs due to the three-point bending load and δ_{rI} and δ_{rII} are the

CODs due to the cohesive stresses. By solving the stress intensity equilibrium for the three-point bending loads and substituting them into the COD equilibrium, a relationship between the COD and the cohesive stresses is obtained

$$\delta = \frac{1}{E^*}\left[\int_0^a \sigma(a,c)H_{\mathrm{I}}(a,c)\,\mathrm{d}c + i\int_0^a \tau(a,c)H_{\mathrm{II}}(a,c)\,\mathrm{d}c\right] \tag{9}$$

where $\sigma(a,c)$ and $\tau(a,c)$ are cohesive stresses at point c along crack length a, and H_{I} and H_{II} are Green's functions relating the three-point bending load to crack opening displacement.

A constitutive relationship for the material is needed to solve the problem. It is given by an equation relating the COD to the cohesive stresses

$$\sigma = f(\delta_{\mathrm{I}}) \tag{10}$$

$$\tau = f(\delta_{\mathrm{II}}) \tag{11}$$

The bilinear and linear relationships of Fig. 6 were used depending on the location of the cohesive force, either in the mortar, aggregate, or interface phase. Interfacial ultimate tensile and shear stresses and fracture energies found from previous research (Buyukozturk and Hearing, 1996a) were used for propagation in the interface. These constitutive laws were implemented independently; in reality, coupling effects on mixed-mode fracture could exist. By substituting this relationship into the COD/cohesive stress equation the crack opening displacement of eqn (9), $\delta_{\mathrm{I}}(a,x)$ and $\delta_{\mathrm{II}}(a,x)$, can be solved, as illustrated in Fig. 8.

Corresponding cohesive forces found from the constitutive model are compared to assumed initial forces; when the COD and cohesive forces agree, the crack zone is in equilibrium. The external force P and load-line displacement D can be computed.

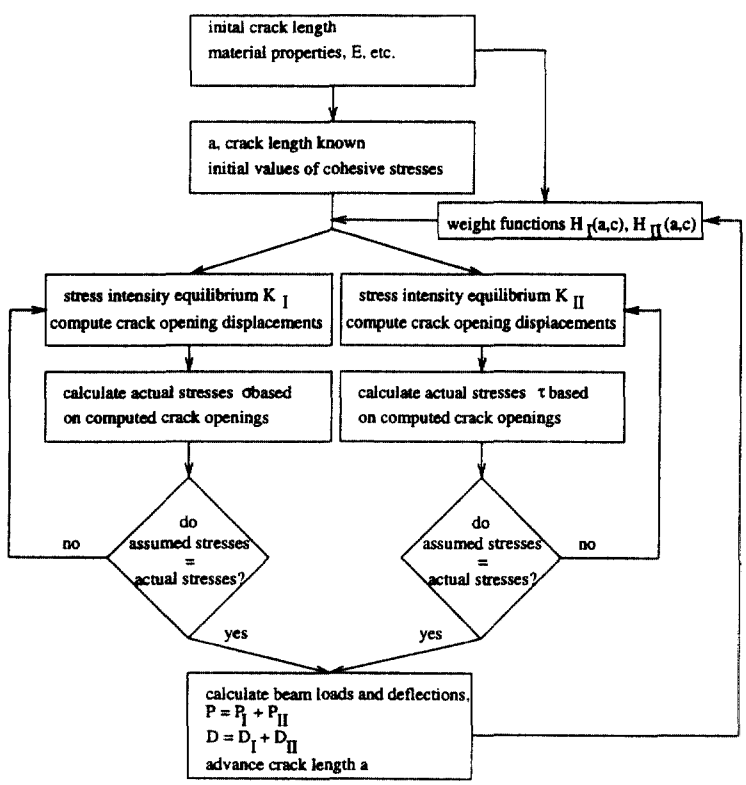

Fig. 8. Flow chart for load/load line displacement numerical procedure.

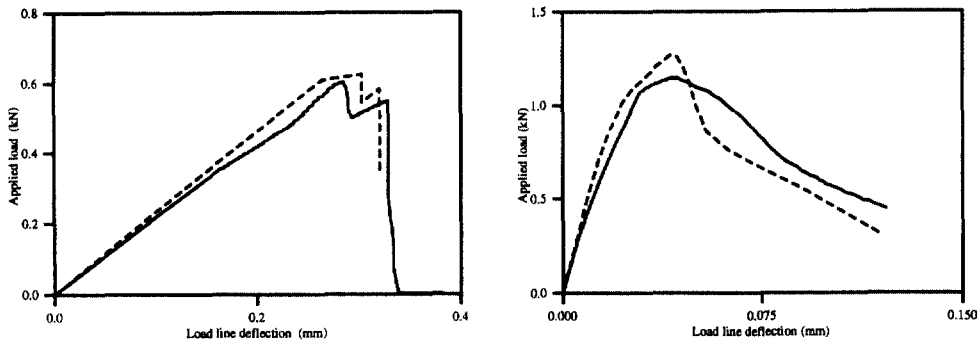

(a) NSM/smooth/1 inclusion (b) HSM/smooth/2 inclusions

Fig. 9. Experimental and numerical load/load-line deflection diagrams.

$$P = P_{\mathrm{I}} + P_{\mathrm{II}} \tag{12}$$

$$D = D_{\mathrm{I}} + D_{\mathrm{II}} \tag{13}$$

Results of analytical models

The load/load-line deflection curves for the three-point bending tests were simulated. From each set of experimental tests a representative sample was chosen to model. Results from sample simulations are shown in Fig. 9. A sample curve from the interfacial fracture simulation is shown in Fig. 9(a) and a sample from the aggregate penetration simulation is shown in Fig. 9(b). The analytical strain–softening model results are plotted with dashed lines while the experimental results are given as solid lines. The results of the simulation programs agree well with the experimental model performance. It is concluded that the method provides accurate results and can be useful to predict the load-displacement behavior of multi-phase composites.

PARAMETRIC STUDY

The analytical models were used to study the effect of material parameters on the composite behavior of the three-point bending specimens. Parametric studies using the models of the interfacial fracture and aggregate penetration fracture scenarios were conducted with variations on relative constituent fracture energies. The influence of the interface fracture energy G_{fi} relative to the mortar fracture energy G_{f_m} as $F_i = G_{fi}/G_{f_m}$ was studied with the interfacial fracture simulation. Numerical simulations with variations of mortar fracture energies were conducted using the interfacial analytical fracture model, shown in Fig. 10(a). Magnifications of the resulting secondary post-peaking behavior are shown in Fig. 10(b). Smaller F_i is shown to result in greater secondary post-peak deflections, indicating that higher relative mortar fracture energies may result in greater ductility in composites with interfacial fracture.

For specimens with aggregate penetration the relative fracture energy of the aggregate G_{f_a} to the mortar G_{f_m} as $F_a = G_{f_a}/G_{f_m}$ was investigated with the aggregate penetration simulation. Analytical simulations with variations of aggregate fracture energies were conducted using the aggregate penetration fracture model. As shown in Fig. 10(c), greater F_a is shown to result in larger deflections, indicating that for transgranular fracture a higher aggregate fracture energy may result in greater composite ductility.

These results illustrate the applicability of cohesive force models to the study of multi-phase composites. It is concluded that in engineering a high performance material for optimum behavior, careful adjustment of the qualities of material constituents can result in improved global material behavior.

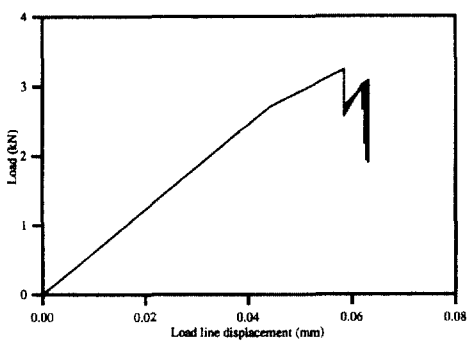

(a) Results of parametric F_i study

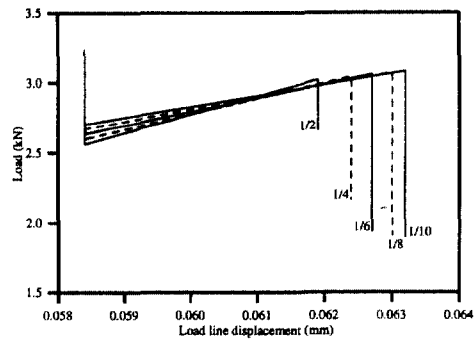

(b) Magnification of post-peak behavior

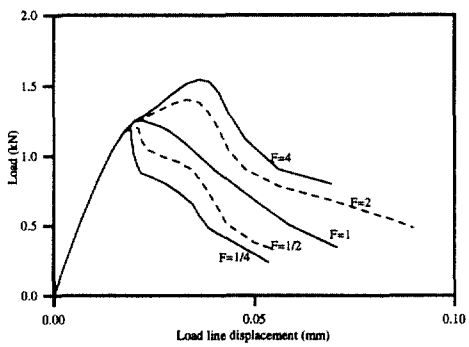

(c) Results of parametric study for parameter F_a

Fig. 10. Results of parametric studies for cohesive model simulations.

CONCLUSION

In this paper, fracture models are presented and a combined numerical/experimental methodology is developed to study the influence of constituent fracture properties on the behavior of concrete composites. Aggregate inclusion specimens are tested to confirm crack-path prediction criteria and to investigate the influence of various combinations of mortars, aggregates, and interfaces. A study is then presented on the influence of relative constituent fracture properties using cohesive force crack propagation models.

From the experimental results, two inclusion specimens are shown to achieve greater ultimate load and ductility with interfacial crack propagation vs aggregate crack penetration. Both cracking scenarios are modeled through cohesive force simulations, and variations of constituent properties are studied. Interfacial fracture simulations showed that a relative increase in mortar fracture energy would improve ductility in composites with interfacial fracture propagation. Similarly, aggregate penetration simulations demonstrate that a relative increase in aggregate fracture energy would improve ductility in composites with aggregate crack penetration.

The methodology developed for the study of crack propagation in cementitious composites is shown to be a suitable approach to the development of high performance concrete with improved ductility and toughness characteristics. Future work will include the extension of these fracture modeling techniques and their results to global material behavior of real concrete, and correlation with experiments on actual concrete specimens.

Acknowledgement—Support of this work was provided by the National Science Foundation through grant no. MSS-9313062. Part of the work reported here includes work performed by Dr Yoshinori Kitsutaka as Postdoctoral Associate at Massachusetts Institute of Technology.

REFERENCES

Buyukozturk, O. (1993) Interface fracture and crack propagation in concrete composites. In *Micromechanics of Concrete and Cementitious Composites*, ed. C. Huet, pp. 203–212. Presses Polytechniques et Universitaires Romandes, Lausanne.

Buyukozturk, O and Hearing, B. (1996a) Constitutive relationships of mortar–aggregate interfaces in high performance concrete. In *Worldwide Advances in Structural Concrete and Masonry*, ed. A. E. Schultz and S. L. McCabe, pp. 452–461. American Society of Civil Engineers, New York, NY.

Buyukozturk, O. and Hearing, B. (1996b) Improving the ductility of high performance concrete through mortar–aggregate interfaces. In *Materials for the New Millenium*, ed. K. P. Chong, pp. 1337–1346. American Society of Civil Engineers, New York, NY.

Buyukozturk, O. and Lee, K. M. (1993) Assessment of interfacial fracture toughness in concrete composites. *Cement and Concrete Composites* **15**(3), 143–151.

Buyukozturk, O., Nilson, A. H. and Slate, F. O. (1971) Stress–strain response and fracture of a concrete model in biaxial loading. *ACI Journal* **68**(8), 590–599.

Carrasquillo, R. L., Nilson, A. H. and Slate, F. O. (1981) Microcracking and behavior of high strength concrete subject to short-term loading. *ACI Journal* **78**(3), 179–186.

Chatterji, S. and Jensen, A. D. (1992) Formation and development of interfacial zones between aggregates and portland cement-based materials. In *Interfaces in Cementitious Composites*, ed. J. C. Maso, pp. 3–12. E & FN Spon (Chapman and Hall), Toulouse.

Dundurs, J. (1969) Edge-bonded dissimilar orthogonal elastic wedges. *Journal of Applied Mechanics* **36,** 650–652.

Foote, R. M. L., Mai, Y.-W. and Cotterell, B. (1986) Crack growth resistance curves in strain–softening materials. *Journal of the Mechanics and Physics of Solids* **34**(6), 593–607.

Gerstle, K. (1979) Material behavior under various types of loading. In *Proceedings of a Workshop on High Strength Concrete*, pp. 43–78. National Science Foundation.

Goldman, A. and Bentur, A. (1989) Bond effects in high-strength silica fume concretes. *ACI Materials Journal* **86**(5), 440–447.

He, M. Y. and Hutchinson, J. W. (1989) Crack deflection at an interface between dissimilar elastic materials. *International Journal of Solids and Structures* **25**(9), 1053–1067.

Hillerborg, A., Modéer, M. and Petersson, P.-E. (1976) Analysis of crack formation and crack growth in concrete by means of fracture mechanics and finite elements. *Cement and Concrete Research* **6**(6), 773.

Hsu, T. T., Slate, F. O., Sturman, G. M. and Winter, G. (1963) Microcracking of plain concrete and the shape of the stress–strain curve. *ACI Journal* **60**(2), 209–223.

Lee, K. M. and Buyukozturk, O. (1994) Fracture mechanics parameters influencing the mechanical properties of high performance concrete. In *Proceedings of the Second International ACI Conference on High Performance Concrete*, pp. 491–498, Singapore.

Lee, K. M., Buyukozturk, O. and Oumera, A. (1992) Fracture analysis of mortar–aggregate interfaces in concrete. *ASCE Journal of Engineering Mechanics* **118**(10), 2031–2047.

Owen, D. R. J. and Fawkes, A. J. (1983) *Engineering Fracture Mechanics: Numerical Methods and Applications*. Pineridge Press Ltd., Swansea.

Rice, J. R. (1988) Elastic fracture concepts for interfacial cracks. *Journal of Applied Mechanics* **55**(1), 98–103.

Romeo, A. and Ballarini, R. (1995) A crack very close to a bimaterial interface. *Journal of Applied Mechanics* **62**(3), 614–619.

Shah, S. P. and Winter, G. (1966) Inelastic behavior and fracture of concrete. In *Causes, Mechanism, and Control of Cracking in Concrete*. SP-20, American Concrete Institute.

Tada, H., Paris, P. C. and Irwin, G. R. (1985) *The Stress Analysis of Cracks Handbook*. 2nd edn. Paris Productions Incorporated, St Louis, Missouri.

Trende, U. and Buyukozturk, O. (1995) Size effect and influence of aggregate roughness in interface fracture of concrete composites. Accepted for publication in *ACI Journal of Materials*.